Reversed flow of Atlantic deep water during the Last Glacial Maximum

Reversed flow of Atlantic deep water during the Last Glacial Maximum

César Negre*, Rainer Zahn, Alexander L. Thomas, Pere Masqué, Gideon M. Henderson, Gema Martínez-Méndez, Ian R. Hall and José L. Mas

*Corresponding Author.

Reversed Atlantic Deep Water Flow During The Last Glacial Maximum

César Negre[1], Rainer Zahn[1,2,3], Alexander L. Thomas[4], Pere Masqué[1,5], Gideon M. Henderson[4], Gema Martínez-Méndez[1], Ian R. Hall[6], José L. Mas[7]

[1]Institut de Ciència i Tecnologia Ambientals (ICTA), Universitat Autònoma de Barcelona, 08193 Bellaterra, Spain (cesar@negre.us)

[2]Institució Catalana de Recerca i Estudis Avançats (ICREA), Lluís Companys 23, 08010 Barcelona, Spain

[3]Departament de Geologia, Universitat Autònoma de Barcelona, 08193 Bellaterra, Spain

[4]Department of Earth Sciences, University of Oxford, Parks Road, Oxford, OX1 3PR, United Kingdom

[5]Departament de Física, Universitat Autònoma de Barcelona, 08193 Bellaterra, Spain

[6]School of Earth and Ocean Sciences, Cardiff University, Main Building, Park Place, Cardiff CF10 3YE, United Kingdom

[7]Dpto. Física Aplicada I. Escuela Universitaria Politécnica (Universidad de Sevilla), Virgen de Africa 7, 41012 Sevilla, Spain

The Atlantic ocean meridional overturning circulation (MOC) is considered to be one of the most important components of the climate system. This is because its warm surface currents, such as the Gulf Stream, redistribute huge amounts of energy from tropical to high latitudes and influence regional weather and climate patterns, while its lower limb ventilates the deep ocean and affects the storage of carbon in the abyss, away from the atmosphere. Despite its significance for future

climate, the operation of the MOC under contrasting climates of the past remains controversial. Nutrient-based proxies[1,2] and recent model simulations[3] indicate that during the Last Glacial Maximum (LGM) the convective activity in the North Atlantic was much weaker than at present. In contrast, rate-sensitive radiogenic $^{231}Pa/^{230}Th$ isotope ratios from the North Atlantic have been interpreted to indicate only minor changes in MOC strength[4,5,6]. Here we show that the basin-scale abyssal circulation of the Atlantic was likely reversed during the LGM and was dominated by northward water flow from the Southern Ocean. These conclusions are based on new high-resolution data from the South Atlantic that establish the north to south gradient in $^{231}Pa/^{230}Th$, and thus the direction of ocean circulation. Our findings are consistent with nutrient-based proxies and argue that further analysis of $^{231}Pa/^{230}Th$ outside the North Atlantic basin will enhance our understanding of past ocean circulation, provided spatial gradients are carefully considered. This broader perspective suggests that the modern pattern of the Atlantic MOC with a prominent southerly flow of deep waters originating in the North Atlantic arose only during the Holocene.

A characteristic feature of our present ocean circulation is the deep convection that occurs in the North Atlantic and spreads North Atlantic Deep Water (NADW) to the world's abyssal ocean. This convection is compensated by the northward flow of warm subtropical surface waters which supply the North Atlantic with large amounts of heat. Changes in MOC therefore carry profound implications for global climate. Information about the operation of the MOC beyond the last 100 years is obtained from palaeoceanographic proxies such as stable carbon isotopes ($\delta^{13}C$) and trace element ratios (Cd/Ca) recorded in the biogenic carbonate of bottom-dwelling foraminifera that trace the

dispersal of biologically cycled nutrients in the ocean. Mapping of these palaeo-hydrographic data suggested that under glacial conditions nutrient-poor NADW ventilated a much smaller fraction of the deep Atlantic, which was dominated by waters from the Southern Ocean[1,2,7]. This is consistent with deep-water temperature, salinity and oxygen reconstructions using independent proxy data and climate modelling[3,8]. These proxies, however, are influenced by deep water circulation and biological nutrient cycling and do not allow a quantitative reconstruction of the abyssal flow rate, which sets marine heat transport and carbon storage.

Information on the abyssal flow rate of MOC can be deduced from the radiogenic isotope pair ^{231}Pa and ^{230}Th in sea-floor sediments[4,9,10]. This is due to their constant production from dissolved uranium at a fixed ^{231}Pa/^{230}Th ratio of 0.093, and their differential solubility in the ocean (more information in supplementary material S1). In their milestone paper Yu *et al.*[4] mapped ^{231}Pa/^{230}Th ratios in Atlantic seafloor sediments and found similar values between LGM and core-top sections, suggesting a southward transport of NADW during the LGM no different from, or possibly even stronger than today. Subsequent ^{231}Pa/^{230}Th records from the North Atlantic have indicated that measurable decreases in overturning occurred during millennial-timescale climate events in the deglaciation but indicate a still vigorous southward flow at the LGM[5,11,12,13]. These findings are in apparent conflict with the mentioned reconstructions derived from nutrient-based proxies[1,2,7].

Interpretation of ^{231}Pa/^{230}Th records in the North Atlantic to date relies on the assumption that the abundance of ^{231}Pa is solely modulated by the southerly flow of NADW, which should cause ^{231}Pa/^{230}Th in the South Atlantic to be higher than in the North[10]. Critical assessment of this interpretation has hitherto been hindered by the lack of continuous fine-scale ^{231}Pa/^{230}Th records from the South Atlantic. Here we present

such a record measured at multi-centennial resolution in a sediment core recovered from the Cape Basin (core MD02-2594; 34º43' S, 17º20' E). At a water depth of 2,440 m, the site is positioned in the present-day flow path of NADW and its southerly position makes it particularly appropriate. To further constrain its $^{231}Pa/^{230}Th$ interpretation, a series of complementary proxies were measured in MD02-2594 (Fig. 1): benthic $\delta^{18}O$ for stratigraphic reference; benthic $\delta^{13}C$ as an indicator of the nutrient content of ambient waters and chemical ventilation; sortable silt mean grain size ($\overline{SS}$) as a measure of near-bottom physical flow speed[14]; and opal concentrations for control on ^{231}Pa scavenging by variable biogenic silica flux[15,16]. Similar analyses were performed on cores further south to serve as reference for constraining $^{231}Pa/^{230}Th$ imprints of deep waters originating in the Southern Ocean (see supplementary information S3).

The $^{231}Pa/^{230}Th$ ratios of core MD02-2594 display a pronounced increase from glacial values of 0.045 ± 0.005 (45-18 ka BP, n=15, 1σ) to Holocene values of 0.065 ± 0.007 (10 ka BP to present, n=15). Such a shift is not observed in the associated data profiles of lithogenic sedimentation rate, authigenic U or opal flux which argues against an imprint on the $^{231}Pa/^{230}Th$ profile by variable lithogenic flux or biological productivity. A prominent decrease is displayed by the total vertical particle flux (*Fv*) going into the Holocene as $^{231}Pa/^{230}Th$ ratios increase. Therefore the $^{231}Pa/^{230}Th$ profile in this core primarily reflects ^{231}Pa enrichment and depletion driven by changes of deep Atlantic circulation. Benthic $\delta^{13}C$ and $\overline{SS}$ profiles from MD02-2594 display a clear glacial-interglacial shift and support a major change in the basin-scale deep Atlantic circulation.

We assess the basin-scale abyssal flow by comparing our record with existing $^{231}Pa/^{230}Th$ profiles from North Atlantic sites (Fig. 2). For this we use a composite record of OCE326-GGC5 (33º42'N, 57º35'W, 4,550 m)[5] and SU90-44 (50º01'N, 17º06'W, 4,279 m)[13] that are positioned along the present NADW path upstream from MD02-2594.

Comparison of late Holocene sections of the records (last 1.5 kyr) show a $^{231}Pa/^{230}Th$ increase from the North Atlantic (0.055 ± 0.002, *n*=4) to the South (0.064 ± 0.002, *n*=3), reflecting ^{231}Pa advection with the southward flow of NADW. Applying a simple radiogenic isotope bottom water flow model[17] this late Holocene $^{231}Pa/^{230}Th$ gradient yields transit time estimates (TTE) of 70 ± 30 years for NADW to travel between 40ºN and 35ºS. These TTE might be an underestimation due to any resetting of the $^{231}Pa/^{230}Th$ signal by opal scavenging as waters pass the productive belt at the equator, but recent work indicates that any such preferential Pa scavenging is minor in this setting during the late Holocene[18]. Indeed, the TTE value fits well with modern CFC-based observations[19].

At the LGM (24-18 ka BP) the situation is fundamentally different and the $^{231}Pa/^{230}Th$ gradient between the South and North Atlantic is reversed. Core MD02-2594 displays $^{231}Pa/^{230}Th$ ratios substantially lower than those in equivalent sections of the North Atlantic records, resulting in a meridional $^{231}Pa/^{230}Th$ gradient that increases toward the north (see Fig. S4-1 for additional data from the equatorial Atlantic[18]). The low values at MD02-2594 also contrast with high $^{231}Pa/^{230}Th$ ratios, well above the production ratio, in sediments from the Southern Ocean that reflect ^{231}Pa enrichment due to scavenging by biogenic opal[4,16,20]. Such a scavenging signal is also represented in our companion record from the southern Agulhas Plateau that was close to but not directly within the northward shifted opal belt of the LGM Southern Ocean (Fig. S3-2).

The MD02-2594 $^{231}Pa/^{230}Th$ ratios hence reflect the presence of abyssal waters low in ^{231}Pa, due to opal scavenging[21], that leave the Southern Ocean to ventilate the deep Atlantic. Sedimentary $^{231}Pa/^{230}Th$ ratios at the LGM that are below production ratio at North Atlantic sites, previously interpreted to reflect vigorous flow from North Atlantic sources[4,5,6] are, instead, due to this northward flow of low ^{231}Pa waters. Our interpretation is consistent with the indication that nutrient-rich bottom waters were present at deep

core sites in both the South and North Atlantic at the LGM[1,2,7]. Previous $^{231}Pa/^{230}Th$ interpretations did not consider the effect of ^{231}Pa scavenging in the Southern Ocean on the ^{231}Pa imprint of southern-sourced waters[4,5] and therefore overestimated deep ventilation from North Atlantic sources under full-glacial conditions. The meridional $^{231}Pa/^{230}Th$ gradient of ~0.03 at the LGM is somewhat larger than the (reverse) gradient seen during the Holocene and suggests a flow from the Cape Basin to the North Atlantic at about half the rate seen in the opposite direction during the Holocene (Fig. 3). A reduced MOC vigour during the LGM is consistent with recent transient atmosphere-ocean model simulations[22] while increased seawater salinity (due to enhanced sea ice formation) stimulated deep water convection in the Southern Ocean hence promoting a flow from the south and driving the LGM abyssal flow reversal[3].

Along Termination 1 (18-10 ka BP), the South Atlantic $^{231}Pa/^{230}Th$ record displays a rather gradual increase that runs opposite to the North Atlantic profiles (Fig. 2). The only measurable step increase at our site is recorded immediately prior to the Heinrich 1 (H1) meltwater event in the North Atlantic. However, the coeval and more accentuated $^{231}Pa/^{230}Th$ shifts at the North Atlantic sites result in a steepened meridional gradient of 0.04 units during H1. While the $^{231}Pa/^{230}Th$ recorded in core GGC5 during H1[5] may be compromised by enhanced biogenic opal deposition[23,24], $^{231}Pa/^{230}Th$ ratios in the subpolar North Atlantic likewise reached values close to the production ratio with low opal fluxes[12,13]. These high ratios would thus reflect a weakening in the northward flow of the MOC, consistent with benthic $\delta^{13}C$, Cd/Ca and Nd isotope fingerprints in the subtropical North Atlantic that indicate the presence of waters from the south at this time[6,25]. During the Bølling-Allerød warm period (14.5-12.8 ka BP), $^{231}Pa/^{230}Th$ and benthic $\delta^{13}C$ in MD02-2594 close to glacial levels still suggest a deep flow dominated by ^{231}Pa depleted SCW. However, North and South Atlantic core sites at this time were

bathed by different water masses due to strengthened NADW production[25] and hence the meridional $^{231}Pa/^{230}Th$ gradient in this period is not diagnostic of the basin-scale abyssal flow vigour. A resumption of SCW is indicated by nutrient proxy records in the subtropical North Atlantic during the subsequent Younger Dryas (YD) cold event (12.8-11.5 ka BP). The meridional $^{231}Pa/^{230}Th$ distribution here suggests that the MOC dropped back to a mode and vigour similar to the LGM. The absence of any larger-scale shifts in our $^{231}Pa/^{230}Th$ profile though the deglaciation suggests that transient episodes of changing convective activity at the northern water mass sources were not strong enough to allow the NADW flow to overcome SCW in the South Atlantic and impact $^{231}Pa/^{230}Th$ at MD02-2594 site, confirming numerical tracer simulations[26].

Within two thousand years of the end of the YD episode the $^{231}Pa/^{230}Th$ ratios from the North and South Atlantic converge. At ~9.7 ka BP, the gradient reverses indicating the establishment of the modern flow pattern with vigorous basin-scale southward transport of NADW that causes ^{231}Pa enrichment in the South Atlantic relative to the North. This is consistent with other proxy data such as benthic Cd/Ca and $\delta^{13}C$[25] as well as Nd isotopes[6,27] that all indicate enhanced ventilation by a nutrient-depleted well oxygenated water mass. Near-bottom physical flow speeds also reach interglacial levels at this time as is indicated by sedimentary $\overline{SS}$ in core MD02-2594 (Fig. 1), marking the retraction of SCW as the prominent source for deep ventilation of the South Atlantic. Atmospheric ^{14}C activities reach full-interglacial levels[28] indicating ancient carbon was completely flushed from the ocean abyssal carbon reservoir due to the accelerated deep ventilation from North Atlantic sources. According to the $^{231}Pa/^{230}Th$ profiles, NADW advection to the south has remained an uninterrupted feature over the whole Holocene period (0-10 ka BP) with average TTE of 130 ± 60 years between 40ºN and 35ºS.

There are several implications to be drawn from the new $^{231}Pa/^{230}Th$ profile from the South Atlantic. Firstly, our data strongly suggest the North Atlantic $^{231}Pa/^{230}Th$ ratios at the LGM reflect the flow of abyssal waters from the Southern Ocean to the north, rather than a southward flow from North Atlantic sources as suggested before[4,5]. Secondly, the LGM $^{231}Pa/^{230}Th$ gradient between our South Atlantic profile and published records from the North Atlantic is consistent with southern-sourced waters flowing northward at a rate about half the average southward flowing NADW during the Holocene. This less vigorous deep flow is in agreement with recent numerical simulations[22]. Finally, the absence of a $^{231}Pa/^{230}Th$ response in our profile to the MOC ups and downs forced by freshwater perturbations in the North Atlantic during the deglaciation supports tracer simulations[26] that demonstrate the insensitivity of our the South Atlantic site to transient perturbation in the north. This therefore confirms that the progressive increase of $^{231}Pa/^{230}Th$ ratios seen in our profile from LGM to the Holocene documents a longer-lasting reorganisation of Atlantic circulation. It has previously been suggested that increased seawater salinity in the Southern Ocean[8] in combination with surface-ocean cooling at the LGM should have stimulated enhanced convective activity at southern sources hence potentially favouring a reversed deep abyssal flow[3,22]. The prominent northward flow documented in the reversed $^{231}Pa/^{230}Th$ gradient at the LGM confirms these predictions and is relevant for understanding the sensitivity of the thermohaline circulation and for the calibration of climate models.

Methods Summary

For the determination of $^{231}Pa/^{230}Th$, sediments were spiked and microwave-digested in a mixture of HNO_3/HCl/HF and cleaned up with reverse aqua regia. Pa, Th and U were separated from each other using Dowex AG1-X8 resin, and isotope abundances were

measured with a Nu instruments MC-ICPMS. In run uncertainties (1σ) of single measurements were <2% for all isotopes. The chronology of MD02-2594 was established with radiocarbon measurements of mono-specific planktonic foraminiferal samples. Analysis of $\delta^{18}O$ and $\delta^{13}C$ was performed on *F. wuellerstorfi* using a ThermoFinnigan MAT 252 mass spectrometer linked online to a single acid bathCarboKiel-II carbonate preparation device. $\overline{SS}$ measurements were undertaken on the terrigenous sub-fraction using a Coulter Multisizer III. Opal determination procedures followed extraction into Na_2CO_3 quantification by the colorimetric Heteropoly Blue Method. The content of lithogenic material was inferred from ^{232}Th and vertical rain rates of sedimentary constituents and focussing were estimated by ^{230}Th normalisation.

References

1. Curry, W.B. & Oppo, D.W. Glacial water mass geometry and the distribution of $\delta^{13}C$ of ΣCO_2 in the western Atlantic Ocean. *Paleoceanography* **20**, 1017, doi:10.1029/2004PA001021 (2005).
2. Marchitto, T.M. & Broecker, W.S. Deep water mass geometry in the glacial Atlantic ocean: a review of constraints from the paleonutrient proxy Cd/Ca. *Geochem. Geophy. Geosy.* **7**, Q12003 (2006).
3. Liu, Z., Shin, S., Webb, R.S., Lewis, W. & Otto-Bliesner, B.L. Atmospheric CO_2 forcing on glacial thermohaline circulation and climate. *Geophys. Res. Lett.* **32**, L02706, doi:10.1029/2004GL021929 (2005)
4. Yu, E.F., François, R. & Bacon, M.P. Similar rates of modern and last-glacial ocean thermohaline circulation inferred from radiochemical data. *Nature* **379**, 689-694 (1996).

5. McManus, J.F., Francois, R., Gherardi, J.-M., Keigwin, L.D. & Brown-Leger, S. Collapse and rapid resumption of Atlantic meridional circulation linked to deglacial climate changes. *Nature* **428**, 834-837 (2004).
6. Roberts, N.L., Piotrowski, A.M., McManus, J.F. & Keigwin, L.D. Synchronous deglacial overturning and water mass source changes. *Science* **327**, 75-78 (2010).
7. Lynch-Stieglitz, J. *et al.* Atlantic meridional overturning circulation during the Last Glacial Maximum. *Science* **316**, 66-69 (2007).
8. Adkins, J.F., McIntyre, K. & Schrag, D.P. The salinity, temperature, and $\delta^{18}O$ of the glacial deep ocean. *Science* **298**, 1769-1773 (2002)
9. Henderson, G.M. & Anderson, R.F. The U-series toolbox for paleoceanography. *Rev. Mineral. Geochem.* **52**, 493-531 (2003).
10. Marchal, O., Francois, R., Stocker, T.F. & Joos, F. Ocean thermohaline circulation and sedimentary $^{231}Pa/^{230}Th$ ratio. *Paleoceanography* **15**, 625-641 (2000).
11. Gherardi, J.-M. *et al.* Evidence from the Northeastern Atlantic basin for variability in the rate of the meridional overturning circulation through the last deglaciation. *Earth Planet. Sc. Lett.* **240**, 710-723 (2005).
12. Hall, I.R. *et al.* Accelerated drawdown of meridional overturning in the late-glacial Atlantic triggered by transient pre-H event freshwater perturbation. *Geophys. Res. Lett.* **33**, doi:10.1029/2006GL026239 (2006).
13. Gherardi, J.-M. *et al.* Glacial-interglacial circulation changes inferred from $^{231}Pa/^{230}Th$ sedimentary record in the North Atlantic region. *Paleoceanography* **24**, PA2204, doi:10.1029/2008PA001696 (2009).
14. McCave, I.N., Manighetti B. & Robinson, S.G. Sortable silt and fine sediment size/composition slicing: parameters for paleocurrent speed and palaeoceanography. *Paleoceanography* **10**, 593-610 (1995).

15. Chase, Z., Anderson, R.F., Fleisher, M.Q. & Kubik, P.W. The influence of particle composition and particle flux on scavenging of Th, Pa and Be in the ocean. *Earth Planet. Sc. Lett.* **204**, 215-229 (2002).

16. Siddall, M., Henderson, G.M., Edwards, N.R., Frank, M., Müller, S.A., Stocker, T.F. & Joos, F. $^{231}Pa/^{230}Th$ fractionation by ocean transport, biogenic particle flux and particle type. *Earth Planet. Sc. Lett.* **237**, 135-155 (2005).

17. Thomas, A.L., Henderson, G.M. & McCave, I.N. Constant bottom water flow into the Indian Ocean for the past 140 ka indicated by sediment $^{231}Pa/^{230}Th$ ratios. *Paleoceanography* **22**, PA4210, doi:10.1029/2007PA001415 (2007).

18. Bradtmiller, L.I., Anderson, R.F., Fleisher, M.Q. & Burckle, L.H. Opal burial in the equatorial Atlantic Ocean over the last 30 ka: implications for glacial-interglacial changes in the ocean silicon cycle. *Paleoceanography* **22**, 4216, doi:10.1029/2007PA001443 (2007).

19. Huhn, O., Roether, W. & Steinfeldt, R. Age spectra in North Atlantic Deep Water along the South American continental slope, 10ºN-30ºS, based on tracer observations. *Deep-Sea Res. Pt I* **55**, 1252-1276 (2008).

20. Walter, H.-J., Rutgers van der Loeff, M.M. & Hoeltzen, H. Enhanced scavenging of ^{231}Pa relative to ^{230}Th in the South Atlantic south of the Polar Front: Implications for the use of the $^{231}Pa/^{230}Th$ ratio as a paleoproductivity proxy. *Earth Planet. Sc. Lett.* **149**, 85-100 (1997).

21. Thomas, A.L., Henderson, G.M. & Robinson, L.F. Interpretation of the $^{231}Pa/^{230}Th$ paleo circulation proxy: new water-column measurements from the southwest Indian Ocean. *Earth Planet. Sc. Lett.* **241**, 493-504 (2006).

22. Liu, Z. *et al*. Transient simulation of Last Deglacialtion with a new mechanism for Bølling-Allerød warming. *Science* **325**, 310-314 (2009).

23. Keigwin, L.D. & Boyle, E.A. Did North Atlantic overturning halt 17,000 years ago?. *Paleoceanography* **23**, PA1101, doi:10.1029/2007PA001500 (2008).

24. Lippold, J. *et al.* Does sedimentary $^{231}Pa/^{230}Th$ from the Bermuda Rise monitor past Atlantic meridional overturning circulation?. *Geophys. Res. Lett.* **36**, L12601, doi:10.1029/2009GL038068 (2009).

25. Boyle, E.A. & Keigwin, L.D. North Atlantic thermohaline circulation during the past 20,000 years linked to high-latitude surface temperature. *Nature* **330**, 35–40 (1987).

26. Siddall, M. *et al*. Modeling the relationship between $^{231}Pa/^{230}Th$ distribution in North Atlantic sediment and Atlantic meridional overturning circulation. Paleoceanography, **22**, PA2214, doi: 10.1029/2006PA001358 (2007).

27. Piotrowski, A.M., Goldstein, S.L., Hemming, S.R. & Fairbanks, R.G. Temporal relationships of carbon cycling and ocean circulation. *Science* **307**, 1933–1938 (2005).

28. Hughen, K.A. *et al.* ^{14}C activity and global carbon cycle changes over the past 50,000 years. *Science* **303**, 202–207 (2004).

29. Zahn, R. & Stuber, A. Suborbital intermediate water variability inferred from paired benthic foraminiferal Cd/Ca and $\delta^{13}C$ in the tropical West Atlantic and linking with North Atlantic climates. *Earth Planet. Sc. Lett.* **200**, 191-205 (2002).

30. Grootes, P.M. Comparison of the oxygen isotope records from GISP2 and GRIP Greenland ice cores. *Nature* **366**, 552–554 (1993).

Supplementary Information is linked to the online version of the paper at www.nature.com/nature.

Acknowledgements

MD02-2594 and MD02-2588 sediment cores were provided by the International Marine Global Changes program (IMAGES) and the Institute Polaire Français Paul Emile Victor (IPEV). TN057-21 and PS2489-2 samples were supplied by Stephen Barker and Alfredo Martínez-Garcia, respectively. Financial support is acknowledged from the Ministerio de Ciencia e Innovación, Spain, through scholarship AP-2004-4278 to C.N., REN2002-01958 to G.M.M., grant CGL2007-61579/CLI and funds from the Comer Abrupt Climate Change Foundation, USA, to R.Z. P.M. acknowledges the ICREA Academia award by the Generalitat de Catalunya.

Author Contributions R.Z. and I.R.H. participated in the MD128 cruise and retrieved the sediment cores; C.N. and G.M.M. sampled the cores; C.N. processed the samples for $^{231}Pa/^{230}Th$ and opal analyses with help from A.L.T. and J.L.M.; A.L.T., G.M.H. and C.N. performed the Pa/Th/U measurements and data processing; G.M.M. performed foraminiferal $\delta^{18}O$ and $\delta^{13}C$ analyses; I.R.H. provided $\overline{SS}$ data; R.Z. and P.M. designed the study and supervised C.N. during his PhD; C.N. and R.Z. wrote the paper. All authors contributed to the interpretation of the results and provided input on the manuscript.

Author Information Reprints and permissions information is available at npg.nature.com/reprintsandpermissions. The authors declare no competing financial interests. Correspondence and requests for materials should be addressed to C.N. (cesar@negre.us).

Figure 1. Multi-proxy profiles of MD02-2594. Benthic stable isotope records of benthic foraminifera (*F. wuellerstorfi*) for (a) $\delta^{18}O$ (*Uvigerina* scale) and (b) $\delta^{13}C$ (corrected for mean-ocean changes)[29], (c) Sortable Silt mean grain size variance, (d) $^{231}Pa/^{230}Th$, (e) ^{230}Th-normalised total vertical flux of preserved particles (*Fv*), (f) ^{230}Th-normalised lithogenic flux, (g) ^{230}Th-normalised opal flux and, (h) authigenic uranium concentration. The LGM to Holocene increase of sediment focussing (i), which leads to lower exposure of sediment at the core top, less dissolution of opal and therefore less masking of real opal sedimentation, allow us to rule out the possibility of an increase in real opal fluxes that could compromise our interpretation of the $^{231}Pa/^{230}Th$ record. Triangles along the upper x-axis mark ^{14}C ages. Error bars indicate analytical s.d. Vertical shading highlights Holocene (0-10 ka BP), yellow; T1 (10-18 ka BP), white; LGM (18-24 ka BP), blue; glacial stages MIS 2 and late MIS 3, light blue).

Figure 2. MD02-2594 *vs.* North Atlantic records. Multiple proxy records depicting ocean circulation and climatic changes during the last 21 kyr in the Atlantic. (a) sedimentary $^{231}Pa/^{230}Th$ ratios from the Cape Basin (MD02-2594; red; this study), eastern North Atlantic (SU90-44; green)[13], and Bermuda Rise (OCE326-GGC5; blue)[5]. The section 18.6-14.5 ka BP of the OCE326 record that is influenced by opal scavenging[23] is drawn in light gray; (b) *F. wuellerstorfi* $\delta^{13}C$ measured in the Cape Basin (MD02-2594; red; this study) and Bermuda Rise (EN120-GGC1, 33º40'N, 57º37'W, 4,450 m; blue)[25] corrected for mean-ocean changes[29]; (c) benthic Cd/Ca from EN120-GGC1[25]; (d) Nd isotope ratios in the Southeast Atlantic (RC11-83, 40º36'S, 9º48'E, 4,718 m; red)[27] and at Bermuda Rise (OCE326-GGC6, 33º41'N, 57º35'W, 4,541 m; blue)[6]; (e) Atmospheric $\Delta^{14}C$ reconstructed from ODP Site 1002, Cariaco Basin[28]; (f) $\delta^{18}O$ record from GISP2, Greenland, indicating atmospheric temperature

variations[30]. Error bars indicate analytical s.d. Yellow vertical shading highlights the Holocene (0-10 ka BP) and Bølling-Allerød (B-A, 12.8-14.5 ka BP) warm periods; Younger Dryas (YD, 11.5-12.8 ka BP) and Last Glacial Maximum (LGM, 18-24 ka BP) in blue; H1 marks the Heinrich 1 interval (~16.8 ka BP).

Figure 3. Atlantic transit times. $^{231}Pa/^{230}Th$ gradient between MD02-2594 record and a composite of the North Atlantic profiles SU90-44 and GGC5 (right y-axis, gray line). The composite is an average of the two North Atlantic profiles, smoothed by a 5 point window and sampled at the time step of the MD02-2594 profile. For the H1 interval, GGC5 was excluded from the composite due to opal scavenging[23]. The gradient was used to compute transit time estimates (TTE) between the mid-latitude North Atlantic and the Cape Basin in the South Atlantic (left y-axis, red line) using an isotope bottom water flow model[17]. This computation was only performed in periods where the North and South Atlantic sites were bathed by the same water mass, which explains the red line discontinuity. The flow pattern is reversed during the LGM indicating a dominant abyssal water flow from the south to the North Atlantic.

Methods

Radiogenic Isotopes

The analytical procedure for the determination of Pa, Th and U concentrations in sediments followed a recently published protocol[31]. 0.2 g per sample were spiked with ^{236}U, ^{229}Th and ^{233}Pa, and microwave digested with a mixture of concentrated HNO_3/HCl/HF (10:4:6 mL). Solutions were dried and 9 mL of reverse aqua regia added as an additional cleanup step. Fluorides were removed by performing 3 evaporation-dilution steps with HNO_3 and finally converted to 4 mL HNO_3 7.5 M. Pa, Th and U were then separated from each other using Dowex AG1-X8 resin, previously washed with HCl and Milli-Q water and preconditioned with HNO_3 7.5 M, adapting the procedure described in Edwards *et al.*[32]. Sample solutions were load onto the resin, which was washed with additional 4 mL of HNO_3 7.5 M and converted to chloride form with 1.5 mL HCl 6M. Th, Pa and U were then eluted with 6mL of HCl 6 M, HCl 6 M + HF 0.05 M, and Milli-Q water, respectively; the Pa fraction was further purified with a second anion-exchange separation. Isotope abundances (^{230}Th, ^{231}Pa, ^{232}Th and ^{238}U) were measured by MC-ICPMS on a Nu Instruments at Oxford University following standard protocols[21]. In run uncertainties (1σ) of single measurements were <2 % for all isotopes. In the case of Th and U, around 90 % of the uncertainties were derived from the calibration of the ^{229}Th and ^{236}U tracers mixed in Barcelona and used in this study. Reproducibility for the entire procedure (*i.e.*, including any possible sample heterogeneity) is 7.0 % for ^{231}Pa, 1.6 % for ^{230}Th, 4.6 % for ^{232}Th and 2.7 % for ^{238}U.

Excess sedimentary ^{231}Pa and ^{230}Th activities were calculated correcting the total concentration for their detrital and authigenic components (details in supplementary information S2), using a $^{238}U/^{232}Th$ activity ratio in the detrital component of 0.6 ± 0.1[9]. Excess ^{231}Pa and ^{230}Th were finally corrected for decay from its chain

predecessors since the time of sediment deposition (see age model section below). The content of terrigenous material in the sediments was inferred from the concentration of ^{232}Th, which is entirely of lithogenic origin, assuming a ^{232}Th concentration of 10.7 ppm in lithogenic material[33]. Vertical rain rates of sedimentary constituents and sediment focussing were estimated by ^{230}Th normalisation[34].

Chronology

The chronology of core MD02-2594 is based on 11 accelerator mass spectrometry (AMS) radiocarbon measurements[35]. The analyses were performed on mono-specific planktonic foraminiferal samples (*Globorotalia inflata*) containing more than 3 mg of carbonate each. Laboratory sample preparation and ^{14}C measurements were carried out at the National Ocean Sciences Accelerator Mass Spectrometry Facility (NOSAMS) at Woods Hole Oceanographic Institution (WHOI), USA. Radiocarbon ages were corrected applying a reservoir age of 615 ± 52 years[36] and converted to calendar years following Fairbanks *et al.*[37].

1D ^{231}Pa/^{230}Th Model

Deep water mass transit time were estimated from sedimentary ^{231}Pa/^{230}Th ratios using a 1D model developed by Thomas *et al.*[17]. The model is an inherently simplified representation of the processes that influence ^{231}Pa and ^{230}Th scavenging during water mass transit. It divides the ocean into 500 m deep boxes down to 4,000 m water depth, with the surface box determining the production of particles that then settle through the underlying boxes at a typical open ocean carbonate particle flux of 0.06 $gm^{-2}d^{-1}$[38]; distribution coefficients for Pa and Th between particulate and dissolved fractions (Kd) are taken from from Siddall *et al.*[16] on the basis of Chase *et al.*[15].

Stable Isotopes ($\delta^{18}O$ and $\delta^{13}C$)

The method used for analysis of benthic stable isotopes ($\delta^{18}O$ and $\delta^{13}C$) is described in Martínez-Méndez *et al.*[39]. Sediment samples were freeze-dried to facilitate desegregation and to minimise physical damage on microfossils during wet sieving. The samples were sieved over a 63 μm screen to separate the sediment coarse and fine fractions. The fine fraction (<63 μm) was oven-dried at 50 °C, weighed and used for Sortable Silt Mean Grain Size ($\overline{SS}$) analyses (see below). The coarse fraction was used for foraminiferal separation. Between 3 and 7 specimens of the epibenthic foraminifera *Fontbotia wuellerstorfi* were picked from the size fraction 250-315 μm at 10 cm steps. Cleaning procedures prior to stable isotope analysis involved light mechanical crushing under methanol followed by ultrasonication for 10-20 seconds to remove sediment coatings and release possible sediment infill. Stable isotopes were measured with a ThermoFinnigan MAT 252 mass spectrometer linked online to a single acid bath CarboKiel-II carbonate preparation device at Cardiff University. External reproducibility was monitored through repeated measurements of an internal laboratory standard (Solenhofen Limestone) and was 0.07 ‰ for $\delta^{18}O$ and 0.03 ‰ for $\delta^{13}C$. All isotope values are referred to the Vienna Peedee Belemnite scale (VPDB) through calibration to the NBS-19 carbonate standard. Benthic $\delta^{18}O$ values are presented on the *Uvigerina* scale, *i.e.* a value of +0.64 ‰ has been added to each *F. wuellerstorfi* measurement to accommodate the offset of this species from oxygen isotope equilibrium with ambient seawater[40].

Sortable Silt

Prior to $\overline{SS}$ analysis carbonate and biogenic opal were removed from the fine fraction by dissolution in 1M acetic acid solution (48 h at room temperature) and digestion in 2M sodium carbonate solution (85ºC for 5 h), respectively. The $\overline{SS}$ grain size measurements were undertaken on the residual terrigenous sub-fraction using a Coulter Multisizer III[41]. The analytical precision ranges between 1-4 %.

Biogenic Opal

Opal digestion was carried out following a protocol adapted from Mortlock and Froelich[42]. 5 mL of 10 % H_2O_2 was added to 50 mg of sample in order to break down organic matter; after 30 min. additional 5 mL of HCl 1M were added to dissolve carbonates. The tubes were sonicated for 30 min. and after another 30 min., 20 mL of Milli-Q water were added and the tubes centrifuged at 4,500 rpm for 6 min. The tubes were then decanted to discard the supernatant and placed in an oven overnight at 60 ºC to remove moisture. 40 mL of 2M Na_2CO_3 were added to each tube, which were shaked and sonified. The tubes were placed in a constant temperature bath at around 85 ºC to disolve silica. After 2 and 4 h the tubes were shaken and returned to the bath, and after a total of 5 h the tubes were immediately centrifuged for 6 min. at 4,500 rpm. The supernatant was stored for analysis.

Opal analysis was performed using the colorimetric Heteropoly Blue Method adapted from Koroleff[43]. 9.5 mL of Milli-Q water were added to clean polypropylene tubes, together with 0.2 mL of molybdate reagent. After 10 min., 0.2 mL of citric acid and 0.2 mL of amino acid were added and left for another 10 min. Next, 0.1 mL of sample solution was added to each of the tubes and left to react for an hour. Finally, the solutions were transferred to spectrophotometer cells and measured with a Hach Lange

DR2800 spectrophotometer. A blank bracketed every sample and a standard solution was measured to make sure that there was no machine drift during the measurements. Method reproducibility is ~10 %.

31. Negre, C. *et al.* Separation and measurement of Pa, Th, and U isotopes in marine sediments by microwave-assisted digestion and Multiple Collector Inductively Coupled Plasma Mass Spectrometry. *Anal. Chem.* **81**, 1914-1919 (2009).
32. Edwards, R.L., Chen, J.H. & Wasserburg, G.J. ^{238}U-^{234}U ^{230}Th-^{232}Th systematics and the precise measurement of time over the past 500,000 years. *Earth Planet. Sc. Lett.* **81**, 175–192 (1986).
33. Taylor, S.R. & McLennan, S.M. *The Continental Crust: its Composition and Evolution*. Blackwell, Oxford (1985).
34. François, R., Frank, M., Rutgers van der Loeff, M.M. & Bacon, M.P. ^{230}Th normalisation: an essential tool for interpreting sedimentary fluxes during the late Quaternary. *Paleoceanography* **19**, PA1018, doi:10.1029/2003PA000939 (2004).
35. Martínez-Méndez, G. *et al.* Contrasting multi-proxy reconstructions of surface ocean hydrography in the Agulhas Corridor and implications for the Agulhas Leakage during the last 345,000 years. *Paleoceanography*, in revision.
36. Southon, J., Kashgarian, M., Fortugne, M., Metivier, B. & Yim, W.E.-S. Marine reservoir corrections for the Indian Ocean and Southeast Asia. *Radiocarbon* **44**, 167-180 (2002).
37. Fairbanks, R.G. *et al.* Radiocarbon calibration curve spanning 0 to 50,000 years BP based on paired ^{230}Th/^{234}U/^{238}U and ^{14}C dates on pristine corals. *Quaternary Sci. Rev.* **24**, 1781–1796 (2005).

38. Honjo, S. & Manganini, S.J. Annual biogenic particle fluxes to the interior of the North-Atlantic Ocean: Studied at 34-degrees-N 21-degrees-W and 48-degrees-N 21-degrees-W. *Deep-Sea Res. Pt II* **40**, 587-607 (1993).
39. Martínez-Méndez, G., Zahn, R., Hall, I.R., Pena, L.D. & Cacho, I. 345,000-year long multi-proxy records off South Africa document variable contributions of northern versus southern component water to the deep South Atlantic. *Earth Planet. Sc. Lett.* **267**, 309–321 (2008).
40. Shackleton, N.J. (1974). Attainment of isotopic equilibrium between ocean water and the benthonic foraminifera genus Uvigerina: isotopic changes in the ocean during the last glacial. *Colloq. Int. CNRS* **219**, 203-209.
41. Bianchi, G.G., Hall, I.R., McCave, I.N. & Joseph, L. Measurements of the sortable silt current speed proxy using the Sedigraph 5100 and Coulter Multisizer IIe: precision and accuracy. *Sedimentology* **46**, 1001–1014 (1999).
42. Mortlock, R.A. & Froelich, P.N. A simple method for the rapid determination of biogenic opal in pelagic marine sediments. *Deep-Sea Res.* **36**(9), 1415-1426 (1989).
43. Koroleff, F. Determination of silicon. In *Methods of Seawater Analysis*, 2nd ed. Verlag Chemie, Weinheim, 174–183 (1983).

Fig. 1

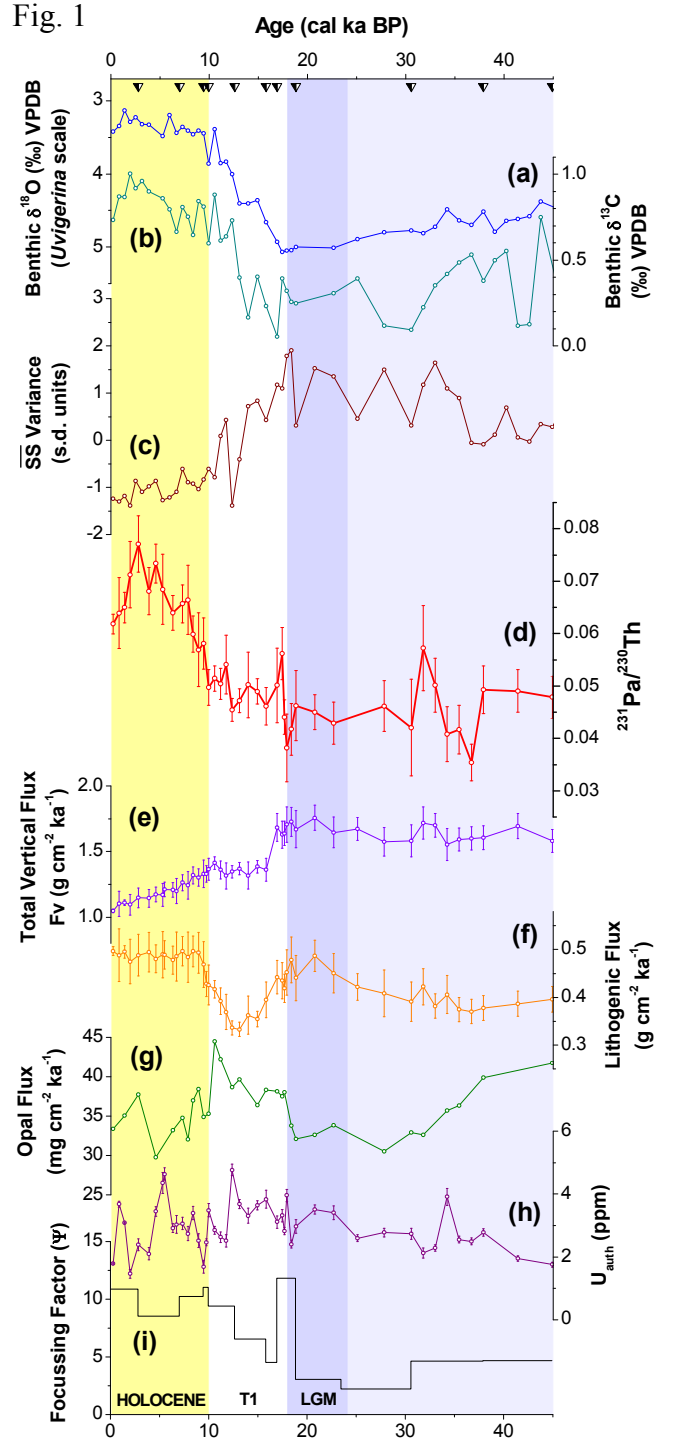
Age (cal ka BP)
0
10
20
30
40
Benthic δ18O (‰) VPDB (Uvigerina scale)
(a)
(b)
Benthic δ13C (‰) VPDB
SS Variance (s.d. units)
(c)
(d)
231Pa/230Th
Total Vertical Flux Fv (g cm-2 ka-1)
(e)
(f)
Lithogenic Flux (g cm-2 ka-1)
Opal Flux (mg cm-2 ka-1)
(g)
(h)
Uauth (ppm)
Focussing Factor (Ψ)
(i)
HOLOCENE
T1
LGM

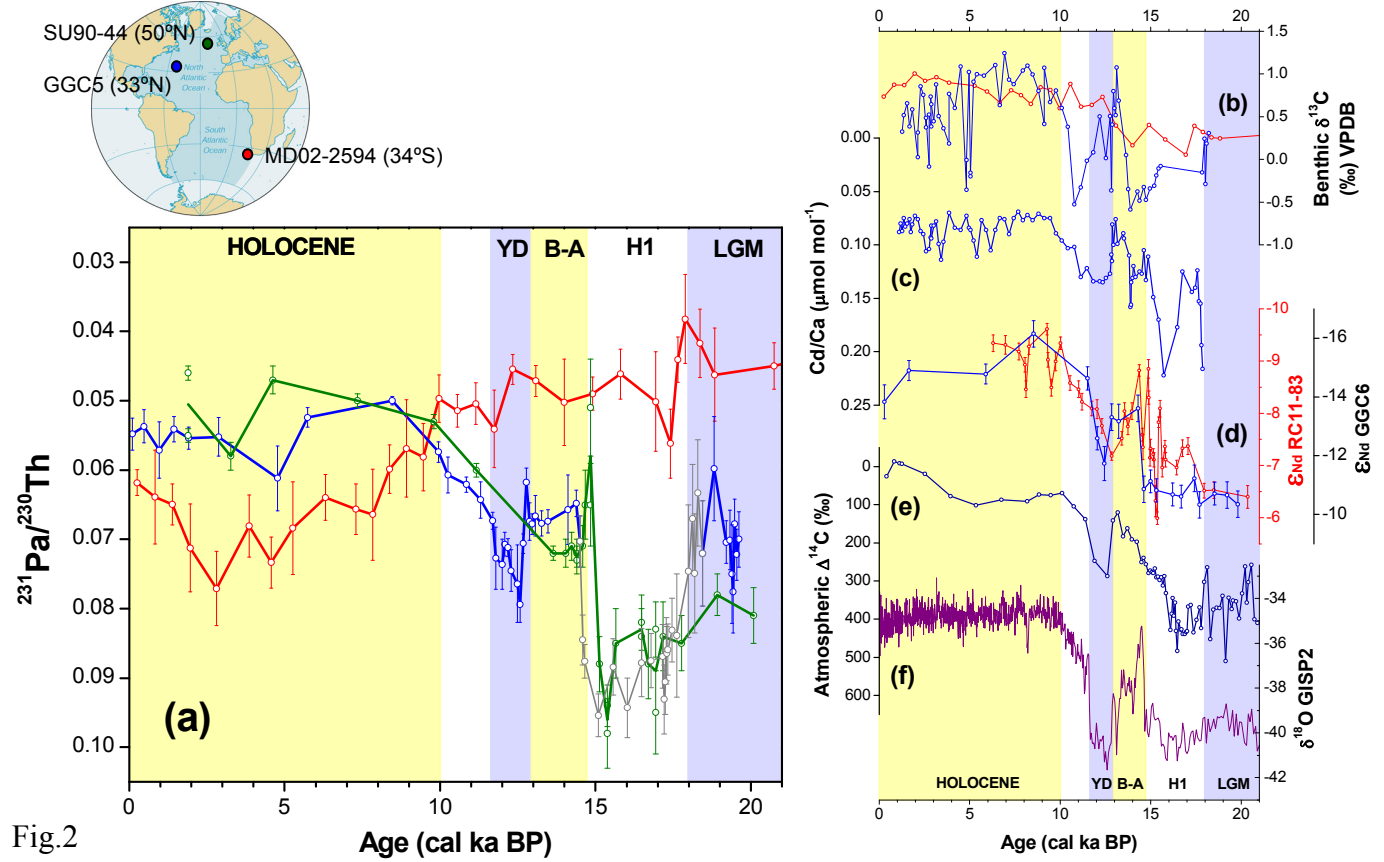
SU90-44 (50°N)
GGC5 (33°N)
MD02-2594 (34°S)
North Atlantic Ocean
South Atlantic Ocean
HOLOCENE
YD
B-A
H1
LGM
(a)
$^{231}Pa/^{230}Th$
Age (cal ka BP)
(b)
Benthic $\delta^{13}C$ (‰) VPDB
(c)
Cd/Ca (μmol mol^{-1})
(d)
ε_{Nd} RC11-83
ε_{Nd} GGC6
(e)
Atmospheric $\Delta^{14}C$ (‰)
(f)
$\delta^{18}O$ GISP2
Age (cal ka BP)

Fig.2

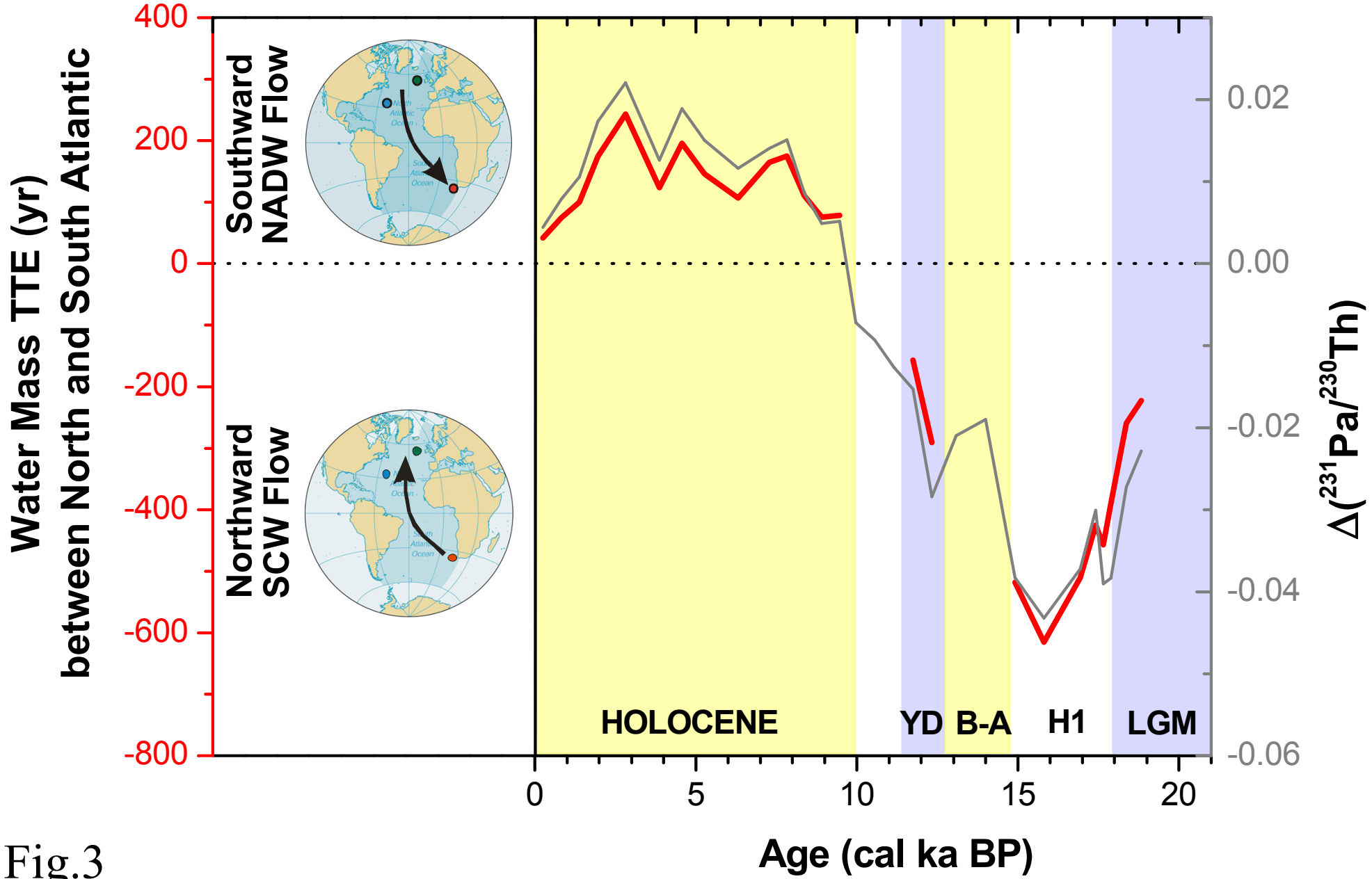
Water Mass TTE (yr)
between North and South Atlantic
400
200
0
-200
-400
-600
-800
Southward
NADW Flow
Northward
SCW Flow
HOLOCENE
YD
B-A
H1
LGM
0
5
10
15
20
Age (cal ka BP)
0.02
0.00
-0.02
-0.04
-0.06
Δ(231Pa/230Th)

Fig.3